Editorial Manager(tm) for Experimental Mechanics
Manuscript Draft

Manuscript Number: EXME784R1

Title: THERMOELASTIC STRESS AND DAMAGE ANALYSIS USING TRANSIENT LOADING

Article Type: Research paper

Keywords: Thermoelastic stress analysis, transient loading, composite materials, damage, delamination

Corresponding Author: Professor Janice M. Barton,

Corresponding Author's Institution: University of Southampton

First Author: Janice M. Barton

Order of Authors: Janice M. Barton; Richard K Fruehmann, BEng MSc; Janice M Dulieu-Barton, BSc PhD; Simon Quinn, BEng PhD

THERMOELASTIC STRESS AND DAMAGE ANALYSIS USING TRANSIENT LOADING

R.K. Fruehmann, J.M. Dulieu-Barton and S.Quinn
School of Engineering Sciences
University of Southampton
Highfield, Southampton, SO17 1BJ, UK

Response to reviewers' comments

We thank the referees for the time they have spent reviewing our paper and for providing us with some helpful comments which have improved the quality of the paper.
We have responded to each comment in turn below and highlighted the manuscript in yellow to indicate where the changes have been made.

Reviewer #1: This papers looks at a variation on thermoelastic stress analysis in which instead of using cyclic loading and lock-in amplification either a single step load or an impact load are used. In either case a dynamic stress field is created, and for short durations the associated thermal problem is approximately adiabatic, resulting in measurable temperature field changes. The point of the work is to demonstrate thermoelastic stress analysis as an NDE technique that might complement or compete with flash thermography or high frequency, vibration induced heating of cracks in structures.

The paper is OK, but could and should be improved.

1. Figures 3 and 4 should have a time scale on them.

Done.

It would also be useful to indicate the framing rate of the IR camera for this data.

Added at top of page 4.

2. There is a difference between the theoretical, TSA, step and impact loading temeperatures, figures 6-9. The authors brush this off as experimental error, but the difference is always there and in the same direction - lower.

We do not brush this off as experimental error. Instead we have provided detailed discussion in the original text as follows:

On the standard test, this is covered on page 8/9 and centres on the assumed emissivity value. The difference in the scatter in the 2.5 Hz and 20 Hz measurement is explained on page 9.

The step loading case in discussed on page 9 and it is highlighted that there is a lower stress limit for which viable readings can be obtained.

For the impulse test (Figs 8 and 9) we say that the difference cannot be attributed to emissivity alone – we highlight potential sources of errors in the clamping arrangement and we mention the possibility of heat dissipation – see bottom of page 10.

It is likely that the process is not entirely fast enough to neglect conduction of heat.

This does not mean that the method will not work, but perhaps the proposed approach must be coupled to transient heat conduction calculations in order to be quantitative about the measured stress levels.

The authors agree with the reviewer's comment that heat transfer is an important consideration when testing at low frequencies, and that this was perhaps not given sufficient emphasis in the original submission. However, in uniaxial tension tests (Figures 6 & 7), where the stress and hence temperature gradients are small (or nominally zero in the UD case), non-adiabatic effects do not provide a sufficient explanation. Hence the experimental errors, for example estimates of the surface emissivity and the material properties (i.e. density, heat capacity, CTE…) are sought to explain the discrepancy (top of page 9). In the bending case (Figures 8 & 9), stress gradients do exist that can account for the larger difference observed and these have been identified in the report at the top of page 11. Clearly this has not been adequately described in the original submission, and therefore Section 4 has been significantly rewritten to provide more clarity to the argument.

In rewriting, the authors noticed that Figure 6 was identical to Figure 7, both showing the data from the LAM specimen. The authors apologise for this mistake and have replaced Figure 6 with the correct data from the UD material. NB The original text actually referred to the correct data!

3. What are the load levels used for the cyclic loading steps of figure 10? What load levels are used to interrogate the samples in order to get the IR images shown?

This has been added to the text on page 11.

Reviewer #2: Well written paper that systematically walks through the methodology and results presented. Discussion of possible reasons for deviations from expected behavior was good. Discussion of how to test for or eliminate these sources of deviation in future work could further enhance the paper.

The results of the bending testing could be strengthened further by verifying the presence of delaminations by additional testing with another nondestructive method such as ultrasonic C-scan, tap test, etc.

In glass fibre reinforced epoxy it is not necessary to do the additional tests as the extent of the damage can be seen visually as shown in Figure 13. We have modified the text on page 13 to clarify this.

Suggested changes to strengthen the paper:
Page 13, paragraph starting at line 7; if the presence/absence of delaminations was verified by another technique (ultrasonic C-scan, tap test, etc) it would strength the results rather than relying solely upon the TSA results presented here, but is not necessary.

See above.

Page 14, paragraph starting at line 5; it seems clear the impact samples were sectioned from the plate samples used in the standard and transient TSA experiments, but it would be more clear if this was stated.

Text has been added on page 13 to clarify.

Figure 2b; Choice of colors makes the measurement position lines somewhat difficult to see, especially for position 1. Suggest that if possible a different color is used for 1, 6 and possibly 8.

WE have changed the figure to make all the lines white.

Figure 8; it is somewhat difficult to see Expt. 5 data points due to the solid vertical grid lines, suggest the the lines are removed or made dashed to make viewing easier.

We have made the gridlines in Figures 8 and 9 fainter.

Submitted 07-06-2009

THERMOELASTIC STRESS AND DAMAGE ANALYSIS USING TRANSIENT LOADING

R.K. Fruehmann, J.M. Dulieu-Barton and S.Quinn
School of Engineering Sciences
University of Southampton
Highfield, Southampton, SO17 1BJ, UK

Abstract

Thermoelastic stress analysis (TSA) is often regarded as a laboratory based technique due to its requirement for a cyclic load. A modified methodology is proposed in which only a single transient load is used for the TSA measurement. Two methods of imparting the transient load are validated against calculations and the conventional TSA approach. Specimens with different damage severities are tested and it is shown that the modified TSA method has the potential to be applied in the field as a non-destructive evaluation tool.

Keywords: Thermoelastic stress analysis, transient loading, composite materials, damage, delamination

1. Introduction

Thermoelastic stress analysis (TSA) is a well established experimental technique [1] for obtaining the surface stress field from a dynamically loaded component. The technique is non-destructive and non-contacting, requiring a minimum of surface preparation ranging from a coating of matt black paint to no preparation at all. As a consequence of the thermoelastic effect a temperature change is induced by dynamic loading, which can be directly related to the stresses. The modern infrared (IR) detectors that are used to measure this temperature change are compact, robust systems that operate in conjunction with a standard PC. The technique therefore offers great potential as a non-destructive strain-based damage assessment tool, which could be used to assess components during routine inspections in the field.

However, the current methodology presents a barrier that has hitherto tethered to the technique to laboratory testing only: the requirement for a cyclic load.

For an orthotropic material under adiabatic conditions, the temperature change (ΔT) related to the change in the stresses by [2]:

$$\Delta T = -\frac{T}{\rho C_p}\left(\alpha_1 \Delta\sigma_1 + \alpha_2 \Delta\sigma_2\right) \quad \textbf{(1)}$$

where T is the absolute temperature, ρ is the density, C_p is the specific heat, α_1 and α_2 are the coefficients of thermal expansion (CTE) in the principal material directions and $\Delta\sigma_1$ and $\Delta\sigma_2$ are the changes in the stresses in the principal material directions .

The thermoelastic temperature change is very small; for example, a typical E-glass / epoxy composite specimen will exhibit a change in temperature of 1.5 mK for an induced stress change of 1 MPa. Modern IR detectors, such as the one used in this work, have a sensitivity of up to 4 mK within a noise of 15 to 20 mK. To increase the thermal resolution, current practice is to subject the specimen to a cyclic load using a servo-hydraulic test machine. This enables the use of a lock-in amplifier (typically using the load cell output as a reference signal) to filter the measured IR signal. The filtered IR signal, typically of 1 to 5 seconds length, is then processed to obtain the amplitude of the thermoelastic temperature change. This filtering and temporal averaging of the IR signal enables stress changes as small as 1 MPa to be resolved.

It is the requirement for a controlled cyclic load and corresponding reference signal that presents a barrier to moving the technique from the laboratory into the field, significantly constraining its application range. The object of this work is therefore to consider a modified approach to TSA that circumvents this barrier. In the proposed new TSA methodology, the component under test is subjected to a single transient load. In the present paper two methods of imparting the transient load into fibre reinforced polymer composite specimens are defined, and underpin the new methodology. The results from the new approach are then validated using both theory and the standard TSA method. Finally the potential of the new TSA

methodology is demonstrated through application to the assessment of damage growth in three different polymer composite laminates.

2. Transient load methodology

The application of TSA using only a single transient load presents two principal challenges. The first is to devise a method of filtering the IR signal. The second is to design a method of introducing a dynamic load into the component of sufficient magnitude to produce a measurable temperature change without the use of laboratory based test machines. In the current work, two methods of imparting a transient load are used. The first uses a servo-hydraulic test machine to apply a uniaxial tension step load to a strip of material. This has the advantage that the load application is controlled and provides easily repeatable conditions for the purpose of evaluation of the technique. The second approach addresses the aim of applying a load without a test machine and is based on a single controlled impact load. A test rig has been designed for this purpose and is based on the application of an impact load to a cantilever beam; the rig is shown in Figure 1. The impact is imparted into the specimen using a pendulum that is released from a known height, thereby providing a repeatable load. The test rig incorporates a mechanism that captures the impactor after the first rebound and prevents repeated loads from being applied. In the current work the magnitude of the applied load is determined by measuring the deflection at the end of the cantilever beam optically from above. However it is possible to incorporate a force transducer in the impactor and this is how the technique would be applied in the field. In the paper the two methods of applying a transient load will be referred to as the ‘step’ and ‘impact’ methods while conventional TSA by means of a cyclic load will be referred to as the ‘standard’ method. The standard, step and impact tests were designed to use the same specimens, which are described in detail in section 4.

To obtain the thermoelastic data from the infra-red detector it is necessary to collect thermal images from test specimens as they are subjected to the transient loading. The temperature

was recorded from approximately one second before the application of the load and for approximately one second after at a frame rate of 383 Hz.

In the step load test the stress field in the specimen and therefore the temperature change field is uniform. Temperature measurements were obtained from a selected area of uniform temperature to give an average surface temperature (T) as shown in Figure 2a. The measurement area comprised 15.5 x 26 mm (30 x 50 pixels). In the impact test the stress varies along the length of the specimen, so transverse lines 20 mm long (40 pixels) were plotted at 10 mm intervals along the length of the specimen, shown in Figure 2b. The average value of temperature from each line plot was used to give T at positions x_1 to x_8 along the length of the cantilever beam.

A typical plot of the surface temperature during a step load test is shown in Figure 3. ΔT (the thermoelastic temperature change) was determined as the difference between the initial and final temperatures (T_1 and T_2), taken to be average values from 50 frames of data just either side of the change in temperature. (Note that a positive, i.e. tensile change in stress results in a negative change in temperature.)

In the impact test (a typical plot is shown in Figure 4) T_1 was also taken as the average of 50 frames of data, but in this case T_2 was taken as the maximum value of the temperature spike. (The measurement was taken on the compressive side of the beam and hence the impact results in a positive temperature change.) The noise in the measurement of ΔT will therefore be larger than for the step method since there is no time averaging of T_2 and a reduced spatial averaging of only 40 sampling points.

This simple combination of temporal and spatial averaging was used to filter the detector output. For example, if the noise were of a Gaussian distribution, 50 sample points would reduce the noise by a factor of 7, as Gaussian `white' noise decreases as the root of the sample size, to give approximately 2.5 mK or one half of the detector sensitivity.

It can be seen in Figure 3 that the response to the step load contains 'noise' with a distinct frequency. The sampling period of 50 frames for T_1 was selected to span a complete number of oscillations, thereby eliminating error associated with averaging over incomplete cycles. The noise is further reduced by the spatial averaging of T, sampled over approximately 1500 points for the step load test and approximately 40 points for the cantilever test. In line with the discussion in the introduction this would give a thermal resolution approximately equal to the detector sensitivity, equivalent to a stress resolution of 3 to 4 MPa. Due to drift in the surface temperature over time, the sample period needs to be kept suitably short. At a detector frame rate of 383 Hz, 50 frames span a period of 0.19 seconds and it can be seen from Figure 3 that the temperature is nearly unchanged over this time period.

This approach differs significantly from standard TSA where proprietary embedded software is used to derive the temperature change data automatically by correlating the thermal data with a reference signal from the test machine. The 'lock-in' procedure rejects signals other than those at the reference frequency; this is not possible when using transient loading.

A flow chart of the methodology used in this paper is shown in Figure 5. To demonstrate that a single transient excitation is sufficient to perform an accurate and repeatable measurement of the stress induced temperature change two validation procedures are carried out shown in boxes 1 and 2 in Figure 5:

1. The measured ΔT values from a step load test are compared with theoretical ΔT values derived from known material properties and the applied stress, and ΔT values obtained from standard TSA using a cyclic load.
2. The ΔT values obtained from an impact test are compared with calculated ΔT values determined from simple bending theory and the known material properties.

The above validations will demonstrate if it is possible to measure reliably and accurately the small stress induced temperature change in a component when only subject to a single

transient load. Furthermore it will allow a comparison between a transient applied by a test machine and that applied by impact loading. This will inform if an impact loading is a suitable for TSA and establish if the technique could be applied in the field for inspection purposes.

Once the viability of the technique has been established the last stage in the methodology is applied and is given in box 3 of Figure 5. Here a stress raiser is introduced into the specimen and both the standard and the two approaches for transient TSA are applied. More damage is evolved by further cyclic loading. The damage is assessed by comparing the data from the damaged and undamaged states.

3. Test specimens and materials

Four material types have been used in the current work: two pre-preg laminates and two resin-infused woven rovings. In all cases the fibre is E-glass. The fibre configuration, laminate stacking sequence and manufacturing process are given in Table 1. Glass-epoxy composites were used as they have a low thermal diffusivity, which means that heat transfer is minimised hence providing a good basis for assessing the transient loading approach.

The unidirectional pre-preg autoclave consolidated material was chosen for two of the specimens (UD and LAM) as autoclaved pre-preg provides the most consistent material properties. The pre-preg material (manufactured by Primco) was cured in an autoclave at 125 °C and 3 bar pressure. The (UD) specimen also has the advantage that the opportunity for heat transfer is reduced further as both the in-plane and through thickness stresses are uniform. The only heat transfer that might take place in this specimen is between the fibres and the resin at the micro-scale, which will not be visible because of the scale of the measurement. The second configuration (LAM) is a $[0, 25, -25, 0]_S$ laminate. The configuration was developed in reference [3], as the ±25° plies were found to encourage delamination under bending loads. Therefore this configuration will be studied without delamination for the validation (see boxes 1 and 2 of Figure 5) of the study and with

delamination for the damage assessment (see box 3 of Figure 5). For both the UD and LAM materials the stress state in the surface ply can be calculated using classical laminate theory (CLT) thereby enabling the calculation of ΔT in the surface ply of the specimens and comparison to the experimentally derived values in the validation part of methodology (see Figure 5 boxes 1 and 2).

The third material type is a plain weave textile composite (WR) that was manufactured by resin infusion with the same $[0, 25, -25, 0]_S$ stacking sequence. The resin was Prime 20 LV with a fast hardener manufactured by Gurit. The consolidation was by liquid resin infusion at room temperature (~20 °C) and atmospheric pressure. The aim was to produce a woven composite with the same favourable delamination behaviour as the pre-preg material for the damage assessment study. The fourth material is a 2 x 2 twill woven composite (TW) with a coarser weave than the plain weave material manufactured with the same resin and identical procedure to WR. This was included to investigate if the influence of the weave pattern on the stress field could be detected using the transient TSA methodology. Local variations in the stress field in the woven materials prevent a simple calculated solution for the stresses from being formulated. Therefore it was decided to use these materials only in the damage assessment (see box 3 of Figure 5).

Material properties for calculating the thermoelastic response based on the known stress in the surface ply were measured using samples of the UD material. The Young's moduli (E_1 and E_2) were obtained from quasi-static tensile tests according to ASTM standard D 3039. The coefficients of thermal expansion (α_1 and α_2) were measured using a strain gauge technique described in reference [4] over the range from 20 to 40 °C. The density (ρ) was measured using microscope images of the material cross-section from several regions cut from a UD specimen and the specific heat capacity (C_p) was measured using differential scanning calorimetry (DSC). The material properties are summarised in Table 2.

Surface preparation is typically not required for epoxy composite materials due to the high emissivity of the material. However, it is important that the surface is matt in order to avoid

reflection sources influencing the measurement. To achieve a matt finish, the surface was lightly abraded by hand using a medium grade 3M Scotch-Brite scouring cloth. This imparts a dull finish to the surface without damaging any of the fibres.

4. Validation of the methodology

Procedure 1

To enable direct comparison between measured and calculated TSA data, the data was converted into a non-dimensional form by taking equation (1) and dividing through by the specimen static temperature (T_1 in the step and impact methods). The calculated non-dimensional temperature change is then given by:

$$\left|\frac{\Delta T}{T}\right| = \frac{1}{\rho C_p}\left[\alpha_1 \Delta\sigma_1 + \alpha_2 \Delta\sigma_2\right] \quad (2)$$

Tests were conducted using the UD and the LAM specimens. Using the material properties in Table 2, the stress state in the surface ply was calculated for six different applied loads corresponding to the stress range in the standard test and the magnitude of the stress change in the transient tests. These varied from 20 to 80 MPa in increments of approximately 12 MPa. To further ensure comparable loading conditions the mean stress was held constant in all the tests. Tests using the standard TSA method were conducted at loading frequencies of 20 Hz (typical test parameter) and 2.5 Hz (comparable to the loading rate of the step load test). Temperature data were collected from the same area of the specimen in each test and the corresponding non-dimensional temperature change was then obtained using equation 2. For the step load method a set of five measurements were obtained at each stress change increment.

Figures 6 and 7 show $\Delta T/T$ data for the UD and LAM specimens respectively for the two standard TSA cases, the step load case and the calculated value of $\Delta T/T$ in the surface ply. For both specimens the standard TSA test at 20 Hz shows good correlation with the calculated values, with a standard deviation in each data point of 1 – 3%. The calculations over predict the measured temperature change from the 20 Hz standard test by approximately 6 % for the

UD and 4 % for the LAM material. The better correlation of the LAM material with calculations may be attributed to small differences in the surface preparation, and a corresponding discrepancy with the emissivity value used in the thermal calibration of the IR data. A value of 0.92 was used for all measurements on the basis of a comparison between two regions of a specimen, one uncoated and one coated with a thin layer of RS matt black paint with a known emissivity of 0.92; the response from the coated and uncoated region was practically identical. Alternatively the small discrepancy could be attributed to errors in the mechanical or thermal material properties (i.e. the density, specific heat capacity and CTE) used in the calculations.

When the loading frequency is reduced to 2.5 Hz Figures 6 and 7 clearly show the correlation between the measured data and the calculated data is not as good as that collected at 20 Hz. The experimental data from the UD material is found to lie between 5 and 12% above the calculated values while the experimental data from the LAM material lies between 15 and 20% below. The standard deviation within each data point is 5 to 8 % for the UD material and 8 to 12% for the LAM material as indicated by the error bars. The only explanation for the larger experimental value from the UD material is an anomaly in the testing. While all tests were conducted in load control, the position amplitude readout at 2.5 Hz was noted on several occasions to be 1% higher than at 20 Hz. The same discrepancy was not noted during the LAM tests. The larger variability in the 2.5 Hz standard TSA measurement compared with the test at 20 Hz can be explained by a decrease in the number of loading cycles included in the TSA measurement; the sampling frequency was kept constant at 383 Hz for all tests, and the sampling duration was approximately 5 seconds for both standard tests.

The step load test, for which only the equivalent of half a loading cycle is available to obtain the measurement, shows a further increase in the standard deviation. At the lowest applied stress change of 22 MPa, the standard deviation is approximately 15% for both materials. This decreases to less than 10% for a stress change of 40 MPa and is comparable to the 2.5

Hz standard test. The tests therefore indicate a lower threshold in transient loading and indicate that a larger applied stress is necessary to obtain a reliable measurement.

The consistently lower values of experimental data compared with the calculations can, in the case of the LAM material, be partially explained by heat transfer between the 0° ply at the surface and the 25° ply below. The stress gradient between the two plies leads to a corresponding temperature gradient (0.010 K mm^{-1} to 0.035 K mm^{-1}). At the reduced loading frequency non-adiabatic conditions result in a reduced thermoelastic response at the surface. Some heat dissipation to the surroundings will also occur, but this is considered negligible at the applied loading rate.

The data clearly indicate that accurate measurements can be obtained using the step load method. The sampling period and the ability to filter the IR data limit the precision of the technique. The minimum required stress change is however slightly higher than predicted. For the technique to be feasible in the field, the method of imparting a load into a component must allow a fast transient which is capable of producing a sufficiently large stress change. In the case of E-glass / epoxy, the minimum stress amplitude needs to be in the range of 40 to 50 MPa, which still lies well below the failure limit of the material.

Procedure 2

The stress field in the cantilever beam was calculated using simple cantilever beam theory and the measured maximum deflection. In the case of the UD material, the force (P) at the free end of the beam is related to the deflection (δz) by the following equation:

$$P = \frac{3(\delta z)E_1 I}{l^3} \quad \textbf{(3)}$$

where I is the second moment of area, E_1 is the Young's modulus in the longitudinal direction and l is the distance from the fixed end to the point at which the force acts. Using the measured deflection, equation (3) was used to calculate the corresponding force at the free end of the beam at the maximum deflection. This could then be used to calculate the stress in the surface ply at any distance (x) from the fixed end using:

$$\sigma_x = \frac{P(l-x)h}{I} \quad \textbf{(4)}$$

where h is half the thickness of the beam. In this case $\Delta\sigma_1 = \sigma_x$ because the beam is initially unloaded. For the UD material $\sigma_2 = 0$. For the LAM material, $E_1 I$ in equation (3) is replaced by the laminate bending stiffness, and instead of equation (4), the bending moment at each distance x was taken and CLT was used to calculate σ_1 and σ_2.

As with procedure 1, the impact test was repeated five times for each material, but only for one pendulum release height. The results are shown in Figure 8 for the UD material and Figure 9 for the LAM material. Notably the experimental data lies below the calculated data by approximately 10 % at the fixed end. The experimental data from both the UD and the LAM specimens show a slightly steeper stress gradient at the fixed end than the calculations. At approximately 20 to 30 mm from the fixed end this then becomes nearly parallel to the line of calculated values.

The uncertainty regarding the emissivity and properties of the material is not sufficient to explain the discrepancy shown in Figures 8 and 9. However, two further effects may explain the lower experimental values. Firstly, bending theory assumes an infinitely stiff clamped end, so flexibility in the clamped end would result in a lower stress, or a longer effective beam length. Secondly, the thin beams have a large through-thickness stress gradient. Although it has been shown that temperature dissipation between plies in specimens loaded in uniaxial tension can be neglected in E-glass / epoxy specimens even at low loading rates [5], large stress gradients exist not only between plies, but also within the surface ply; the stress in the outer surface of the LAM specimen is 25 % greater than the stress at its inner surface. The average surface ply stress is therefore 13 % lower than the surface stress, accounting for a large portion of the discrepancy with the calculations in which the surface stress was used. Furthermore, the stress gradient between the plies is much greater in the bending case than in the uniaxial tension case, and hence some non-adiabatic behaviour between the subsurface

plies my influence the surface temperature change as well. Taking this into account, the calculated and measured stress data correlate very well.

The results from the two validation tests indicate that the modified TSA procedure is a valid approach that can be applied to obtain quantitative measurements. The precision is lower than for a standard test conducted at a higher frequency, and hence the minimum stress change required to obtain a reliable measurement is greater. Also, non-adiabatic effects are a consideration, particularly if the rate of loading is low, as in the examples shown in this work.

5. Damage assessment

The spatial averaging used in the previous section to improve the effective thermal resolution is not practical for the purpose of damage assessment for which full-field data is desired. In the following tests, the method of obtaining ΔT was as described in section 2, except that the temperature measurement was taken on a pixel by pixel basis to provide an image of the non-dimensional ΔT field.

Damage assessment was conducted on three material types, LAM, WR and TW. Two types of specimen were used: two tensile strips as described in section 3 made from the LAM and TW materials, and two plate specimens, nominally 250 x 100 mm, made from the LAM and WR materials.

The tensile specimens were loaded using the step method (LAM) and the impact method (TW). A stress concentration was introduced in the form of a 4 mm diameter hole in the centre of the strip. The specimens were then subjected to a tensile sinusoidal load at constant load amplitude (giving a far field stress of 230 MPa for specimen LAM and 180 MPa for specimen TW) for two sets of 18000 cycles at 2 Hz (specimen LAM failed after 26500 cycles) and a TSA measurement was taken after each set. TSA measurements of both specimens were taken using a stress change of approximately 70 MPa in the far field at 20 Hz.

Figure 10a shows non-dimensional standard TSA data from LAM with no damage (step 1), after zero fatigue cycles but with the stress raiser (step 2), after 18000 fatigue cycles (step 3) through to failure (step 4). At step 4, only a narrow band along the right hand edge of the specimen was still intact, allowing the final TSA measurement to be taken. All TSA data was obtained at the same load amplitude. The corresponding TSA data obtained using the step method is shown in Figure 10b. Note that the standard data gives only a magnitude and hence the compressive regions above and below the hole show as positive values. In the step data which is a simple difference between T_1 and T_2 these regions show a negative temperature change.

Up to step 3, the standard and step method data is very similar. However, at step 4 a very large difference between the standard and step methods is plainly visible. This is due to frictional heating in the damaged regions which accumulates a net increase in the absolute specimen temperature due to the cyclic load. Although this should be accounted for in the non-dimensional data in which ΔT is normalised against the absolute surface temperature, in the example shown in Figure 10a, the heating is so great that the surface temperature exceeds the detector calibration range. By decreasing the detector exposure time, the range can be increased, however, at the expense of a loss in sensitivity. Furthermore, the magnitude of the localised heating may not be known *a priori*.

Using the step load method, the effect of local heating is eliminated because the heat generation is transient and does not have the opportunity to 'accumulate' in the specimen and cause large temperature evolutions. As a consequence, localised heating is minimised. Therefore the remaining load bearing section of the specimen is easily identified in step 4 of Figure 10b along its right hand edge. This result demonstrates that the application of a transient load for TSA based damage assessments has great benefit.

The TW specimen enables a qualitative evaluation the resolution of the TSA transient loading methodology, as the interlacing of the fibres in the textile results in stress concentrations at a small scale. Fatigue of the textile composite leads to a change in the distribution and

magnitude of these stress concentrations. The aim here is therefore to verify if such fine details in the stress field can be resolved using the modified TSA method.

Damage was introduced and progressed in the same way as for the LAM specimen except that the specimen did not reach ultimate failure. The data in Figure 11 shows that the stress concentration around the hole can be identified using the impact method. The deterioration in the weave structure is however not picked up by the impact method to the same extent as by the standard method. A slight decrease in the magnitude of the signal, in particular towards the free end, can be identified. This data shows that further refinement of the technique will be necessary in order to enable small scale features in the stress field to be identified using the impact method.

Next the two plate specimens were tested. The aim of this test was to investigate a more realistic damage case. Delamination damage was introduced into the specimen using a bending rig shown in Figure 12. The curved edge of the clamp introduces a stress concentration in the centre of the plate resulting in a delamination between the ± 25° plies. In the LAM material a significant delamination was obtained after 26500 cycles. The displacement amplitude of the actuator, shown in Figure 12, was 35 mm at a distance of 75 mm from the clamped end. In the WR material, damage was limited to the surface ply as a result of the contact with the clamp, but no delamination was observed, even after 36500 cycles under the same loading conditions as the LAM material. Because a glass fibre epoxy composite was used, it was possible to identify the damage in the two specimens by visual inspection. The damage is shown in Figures 13a and b for the LAM and WR specimens respectively, where a clear subsurface delamination can be identified in the LAM specimen. The damage in the plate specimens was then examined TSA: firstly by testing in tension using the standard and step methods and then using the impact method. For the impact tests, the plates were cut into 25 mm wide strips such that the damaged region was 20 mm away from the clamped section.

Figures 14 and 15 show the TSA data obtained from the tensile tests using the standard (Figures 14a and 15a) and step (Figures 14b and 15b) methods. The surface damage can be identified in both materials, more clearly in the WR material which had more significant surface damage. The extent of the delamination in the LAM cannot be identified in the data from either the standard or the step methods. This implies that a delamination does not influence the stress field in a laminate under in-plane tensile loading and can therefore not be detected by this method. The test does however show that localised fibre breakage in the surface ply (as in the LAM material) can be identified using the step method, although this damage is more clearly visible using the standard method. In both the LAM and the WR materials, the surface damage appears as an area of reduced thermoelastic response. This indicates that the load is being diverted away from the surface ply and into the plies below. Unlike the TW specimen the weave pattern in the WR specimen is not apparent in the data because of the small scale of the weave and the resolution of the detector settings.

The impact test was then conducted to investigate if the delamination damage could be identified in bending. The data from the LAM and WR materials is shown in Figure 16a and b respectively. The data is taken from the compressive side of the specimen where localised buckling might reveal the delamination. However, it is clear from Figure 16 that this is not the case. The data shows only the surface damage. It is however promising that the resolution is comparable to that obtained using the standard and step methods. Also, the asymmetry in the clamping conditions of the LAM specimen can clearly be identified in Figure 16a.

The above investigations of damage progression in a variety of composite materials demonstrate that the modified TSA method has potential to provide information on the stress field in a component in situations where a cyclic load is impractical. This can be due to limited access to loading machines as might be expected outside of the laboratory environment, but also due to the presence of defects that cause localised heating under cyclic loading. The technique also enables greater flexibility in the types of loading scenario to

which a component can be subjected, allowing the extent to which damage in the component influences the stress field in a particular loading case, to be assessed. Further work is required to improve the thermal / stress resolution of the modified technique. Although the general stress field is well captured, finer details in the stress field may not be resolved by the modified method.

6. Conclusions

The results show that quantitative data can be obtained using a single transient load with a comparable accuracy to the standard TSA method. The rate and magnitude of the stress change must exceed a minimum threshold which will vary depending on the material. In the case of E-glass / epoxy composites, relatively low loading rates and magnitudes are sufficient.

With regard to the identification of damage, the technique relies on a stress redistribution in the surface ply. This is no different from the standard method. However, the greater simplicity of the modified technique provides improved flexibility for introducing load into the specimen. The greatest difficulty will always be to generate a realistic loading scenario, and a sufficient load amplitude. Development of the filtering of the thermal data to improve the effective thermal resolution of the technique is required to enable small scale stress concentrations to be identified; these challenges will be the object of future work. The present study has confirmed the feasibility of applying TSA as a damage assessment technique for in-service components. The work represents an important initial step in taking the TSA technique away from the laboratory and opens a new application range of significant industrial relevance.

Acknowledgments

The authors are grateful for the support of the Engineering and Physical Sciences Research Council and Airbus UK.

References

[1] Stanley P., Chan W. K., "Quantitative stress analysis by means of the thermoelastic effect", *Journal of Strain Analysis*, **20**, 129-137, 1985

[2] Stanley P., Chan W. K., "The application of thermoelastic stress analysis techniques to composite materials", *Journal of Strain Analysis*, **23**, 137-143, 1988

[3] Emery T. R., Dulieu-Barton J. M., "Damage monitoring of composite materials using pulsed phase thermography and thermoelastic stress analysis", *Key Engineering Materials*, **347**, 621-626, 2007

[4] Lanza di Scalea F., "Measurement of thermal expansion coefficients of composites using strain gages", *Experimental Mechanics*, **38**, 233-241, 1998

[5] Cunningham P. R., Dulieu-Barton J. M., Shenoi R. A., "Damage location and identification using infra-red thermography and thermoelastic stress analysis", *Proceedings of SPIE*, **4704**, 93-103, 2002

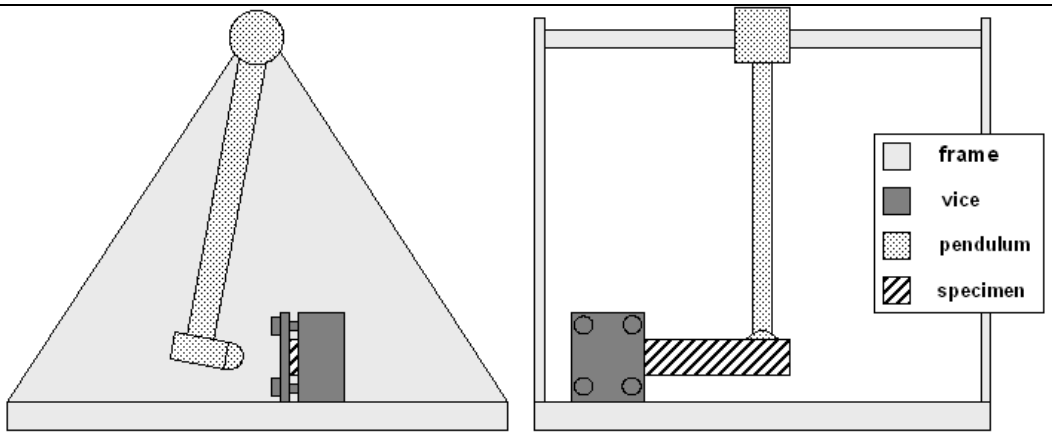

Figure 1: schematic of the impact rig

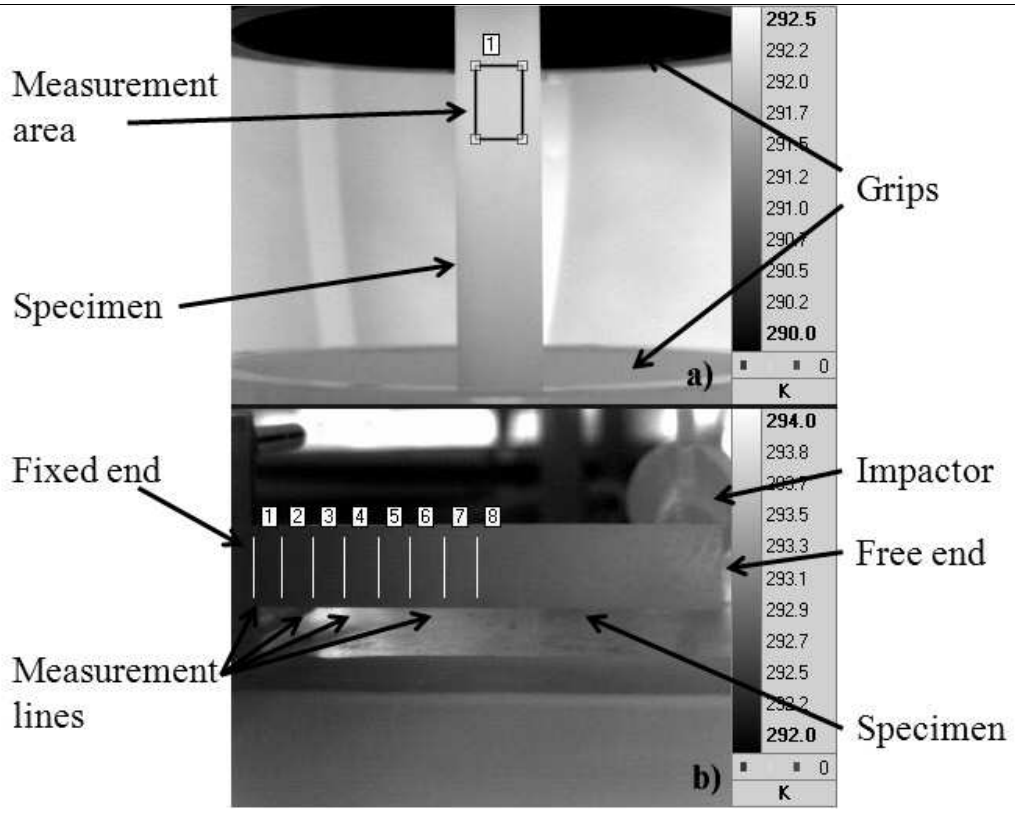

Figure 2: thermal images during a) a step load test, b) a cantilever impact test, showing the positions (area 1 and lines 1 to 8) at which temperature measurements were taken

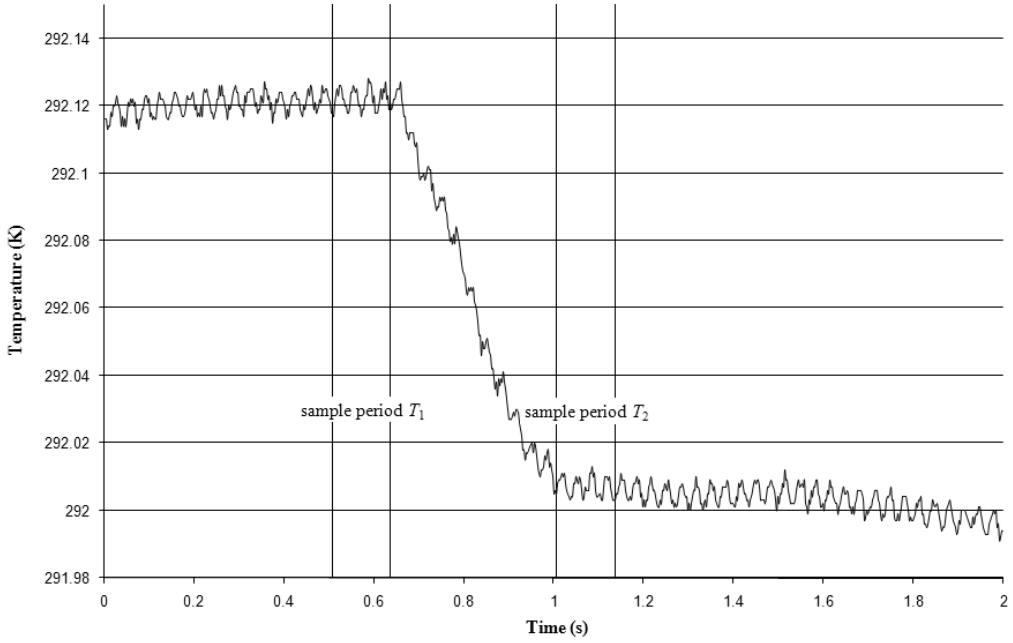

Figure 3: change in temperature during a step increase in load in a uniaxial tensile specimen

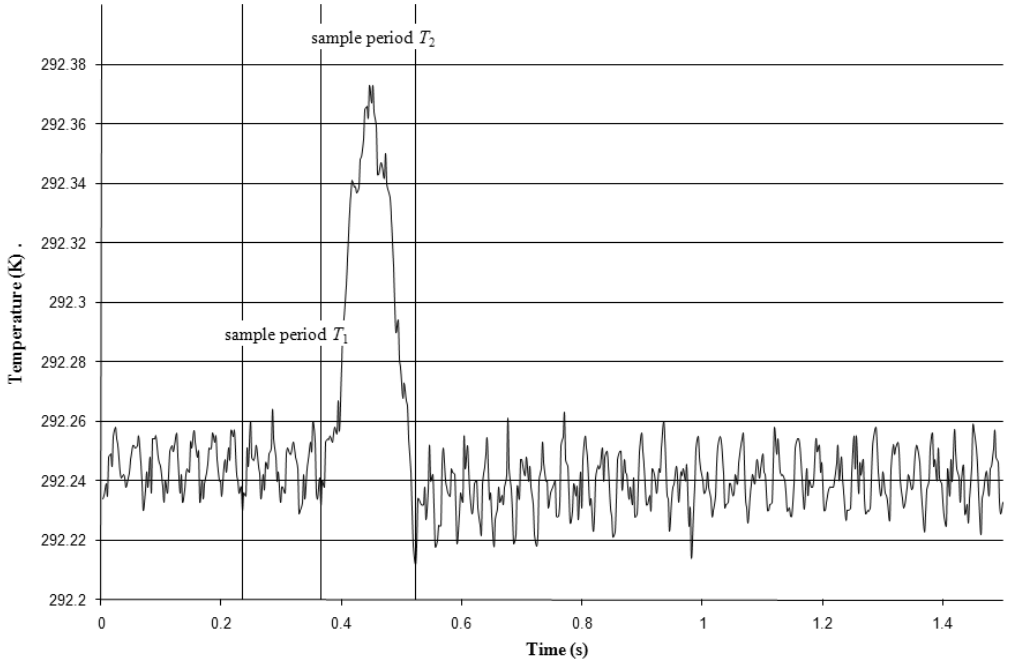

Figure 4: change in temperature during a cantilever impact test

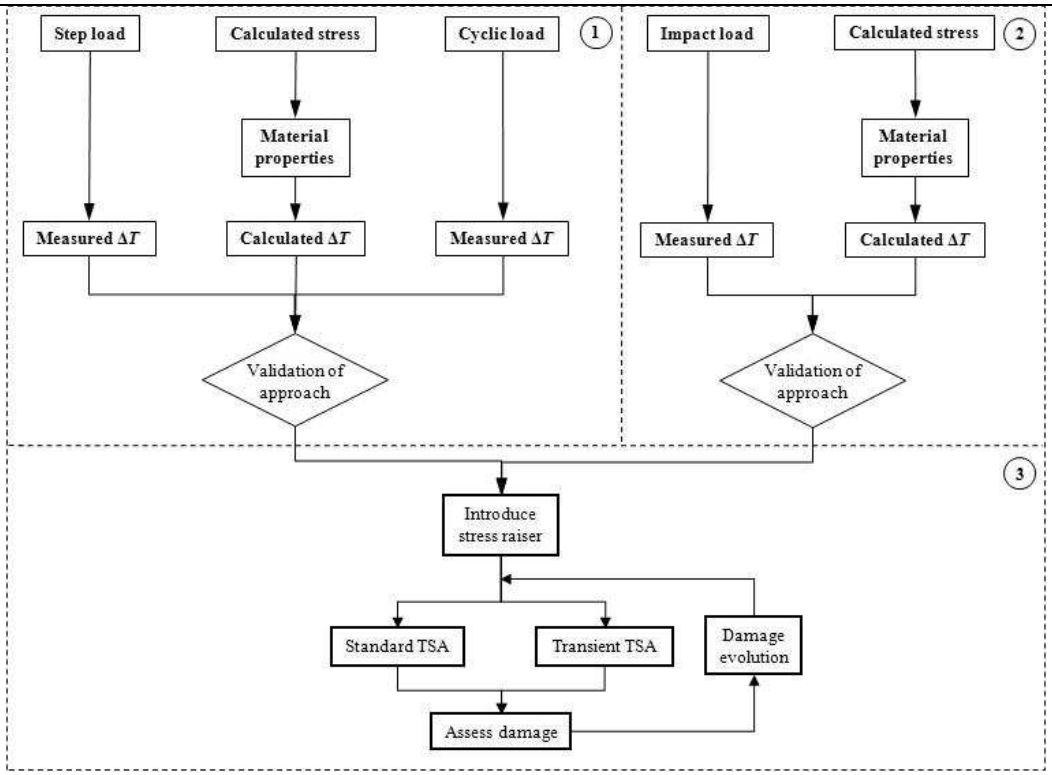

Figure 5: Flowchart of methodology

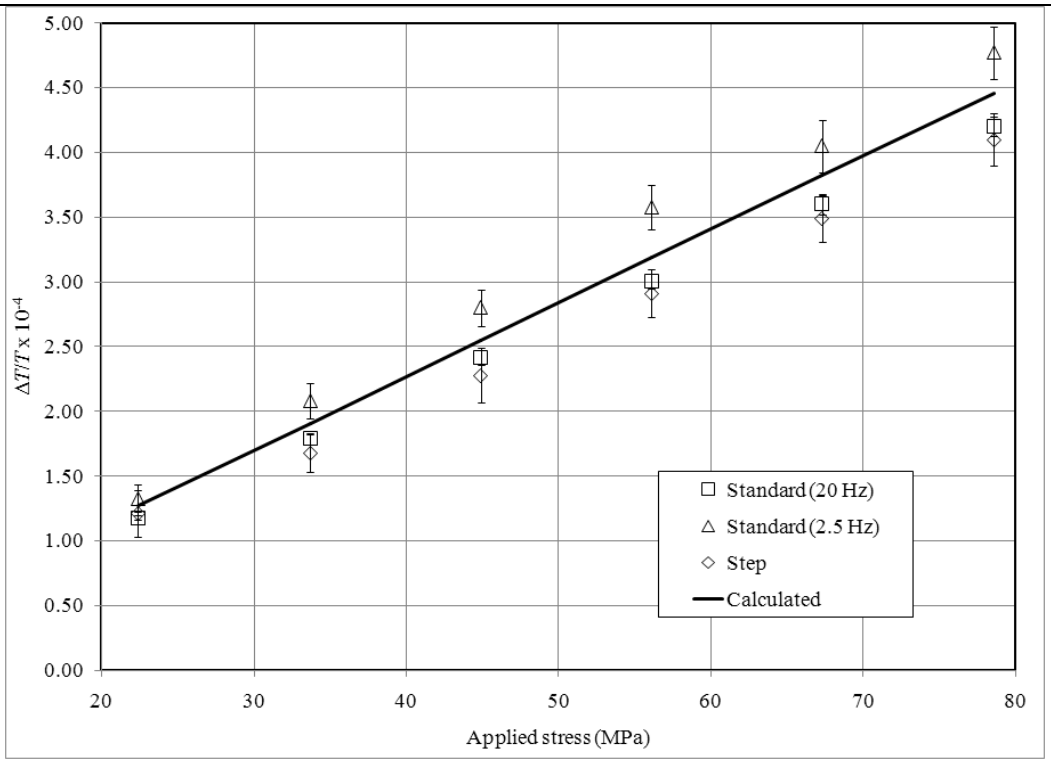

Figure 6: Comparison of the non-dimensional thermoelastic response of a UD tensile strip at different loading amplitudes obtained using the standard and step loading methods

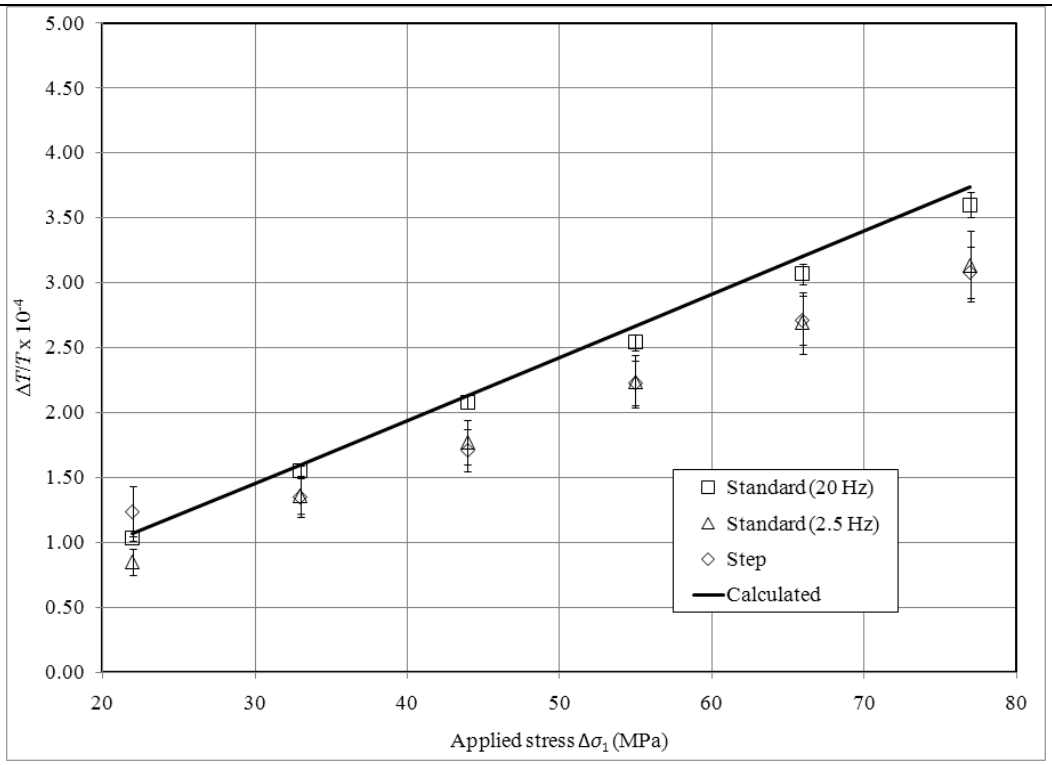

Figure 7: Comparison of the non-dimensional thermoelastic response of a LAM tensile strip at different loads obtained using the standard and step loading methods

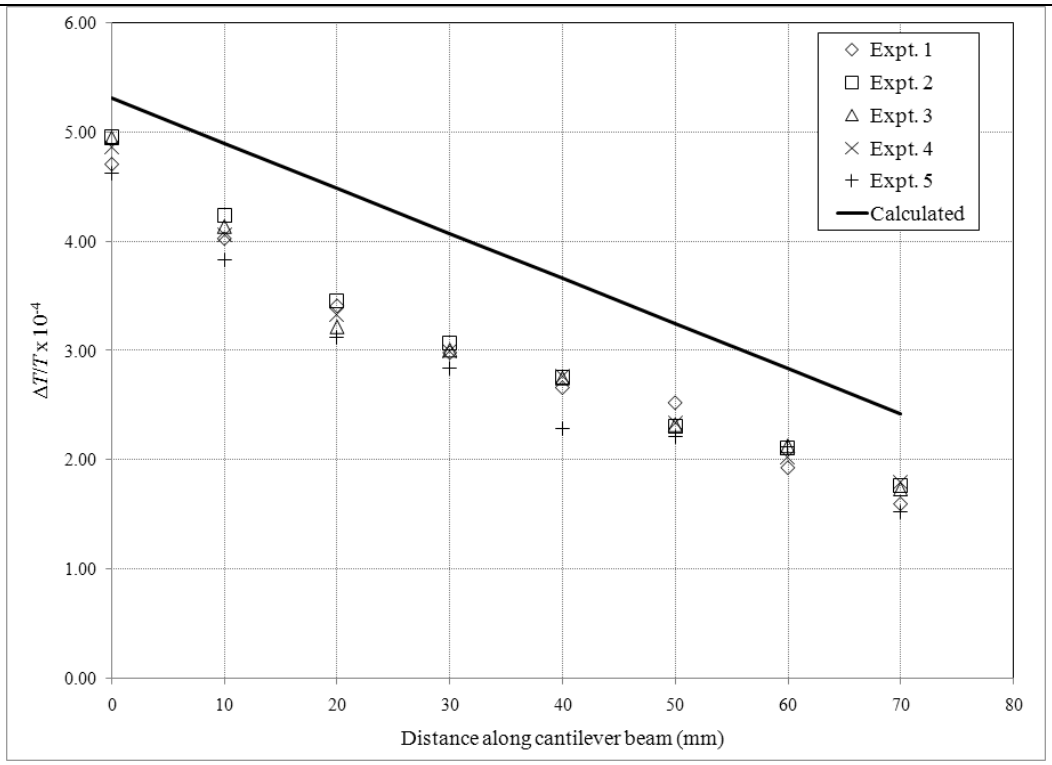

Figure 8: Non-dimensional temperature change distribution in the cantilever beam UD, deflection 17.5 mm

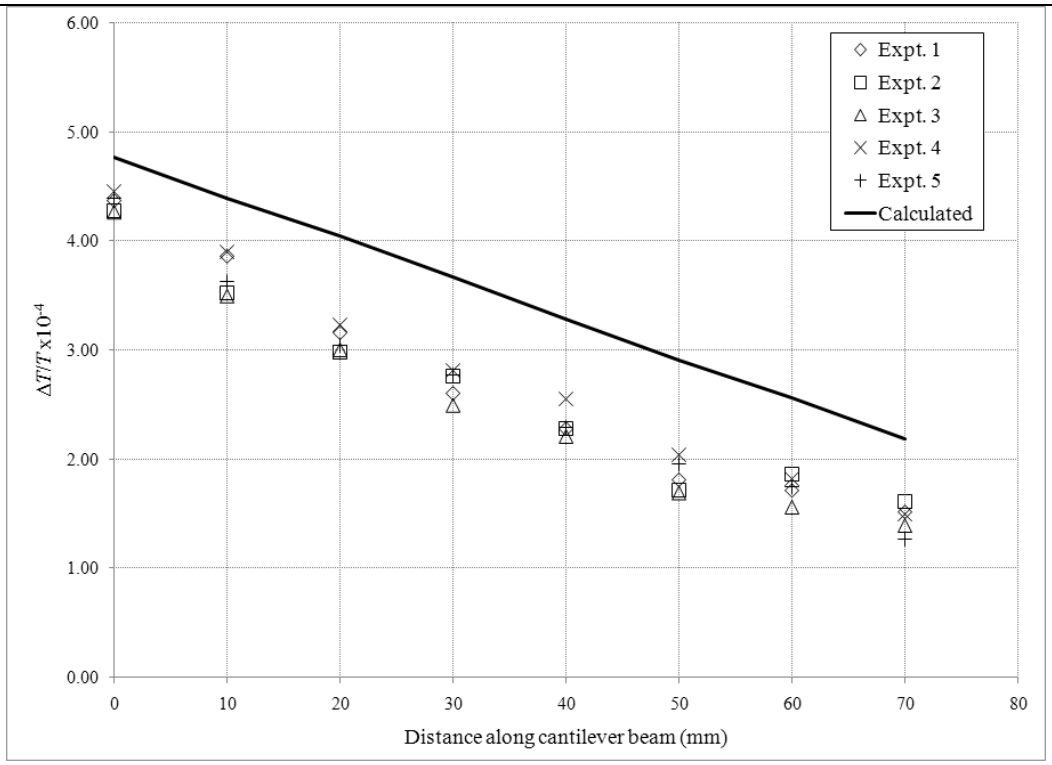

Figure 9: Non-dimensional temperature change distribution in the cantilever beam LAM, deflection 18.2 mm

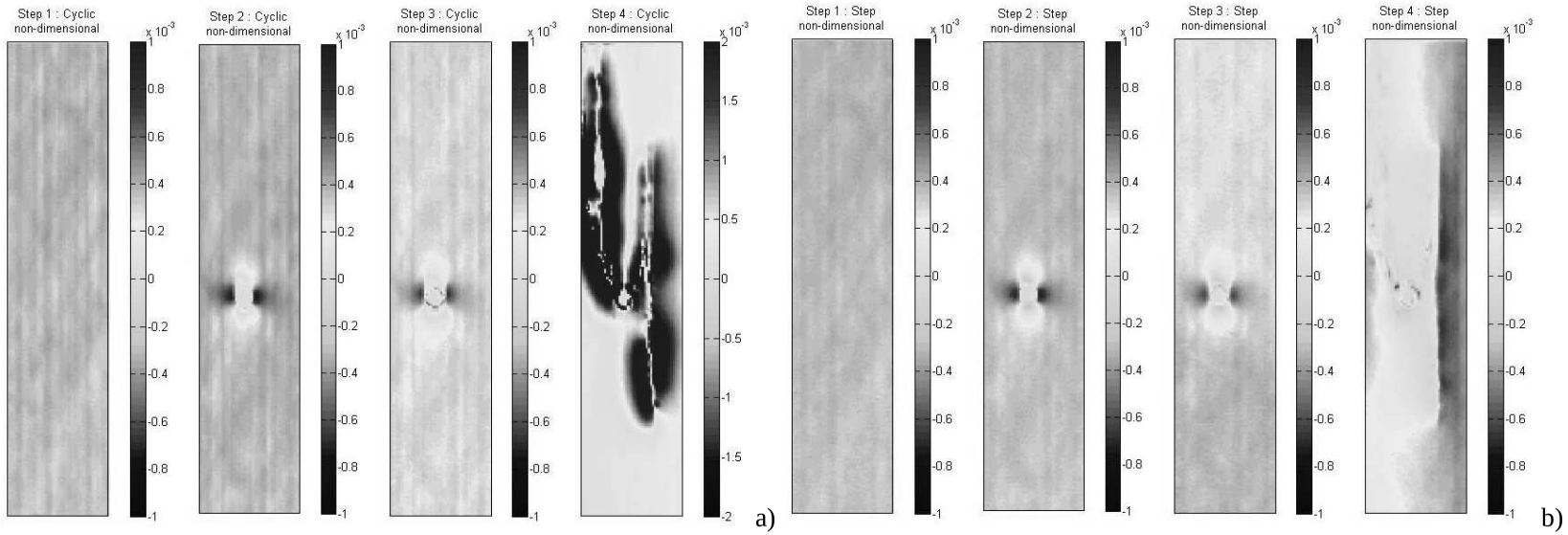

Figure 10: Progression of damage around a hole in the LAM material using a) the standard method and b) the step method

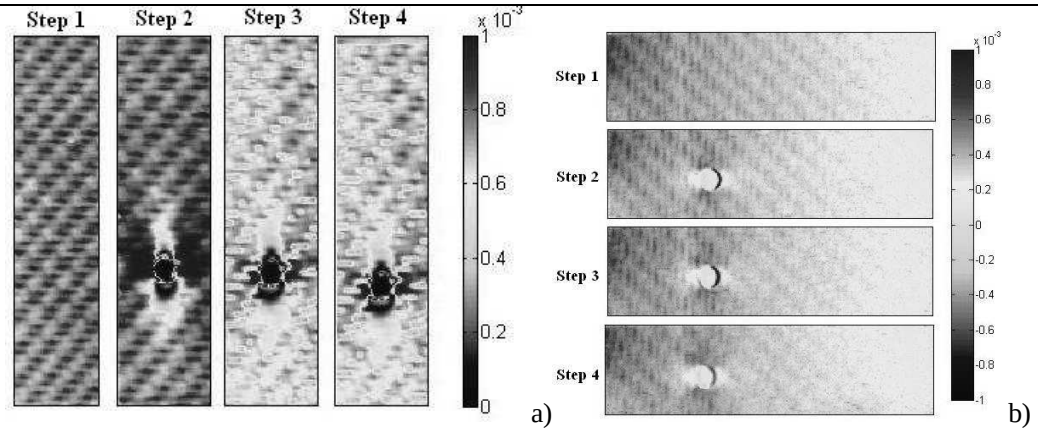

Figure 11: Progression of damage around a hole and within the weave structure in the TW material using a) the standard method and b) the impact method

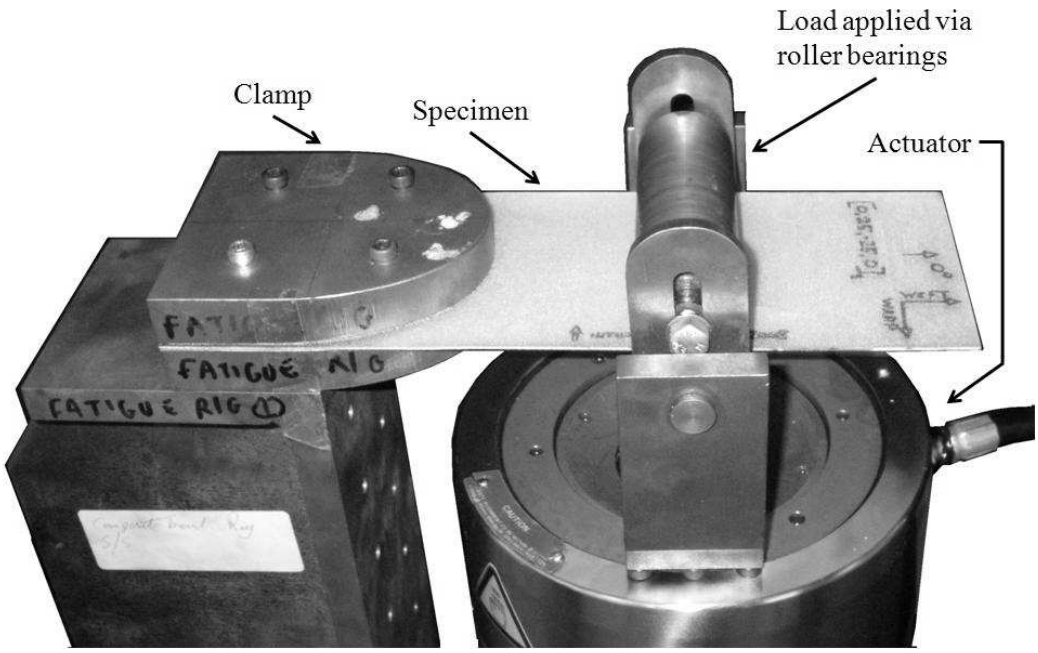

Figure 12: Fatigue loading rig used to introduce damage to the plate specimens

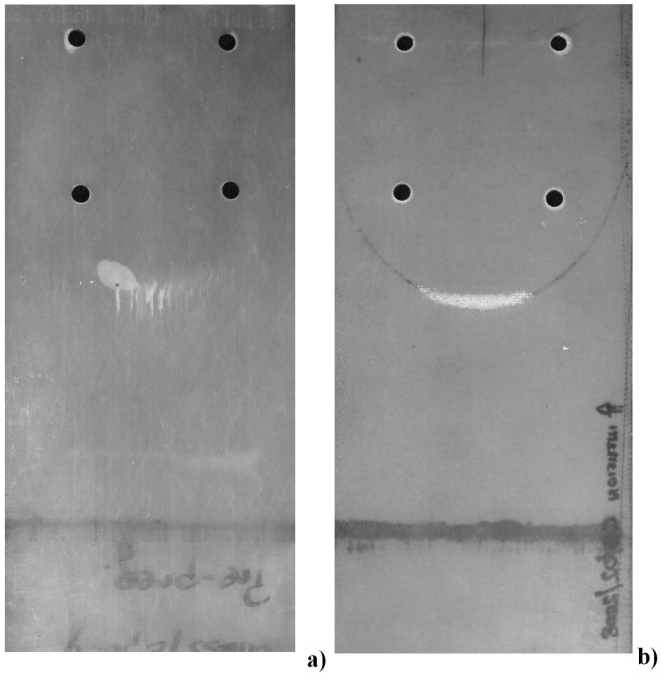

Figure 13: Damage location in a) LAM and b) WR plate specimens

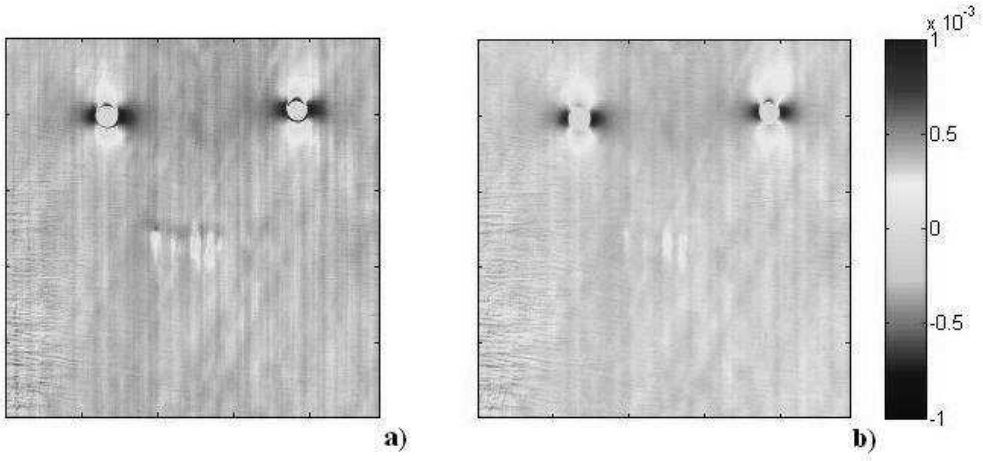

Figure 14: non-dimensional TSA data from damaged LAM plate obtained using a) the standard and b) the step load methods

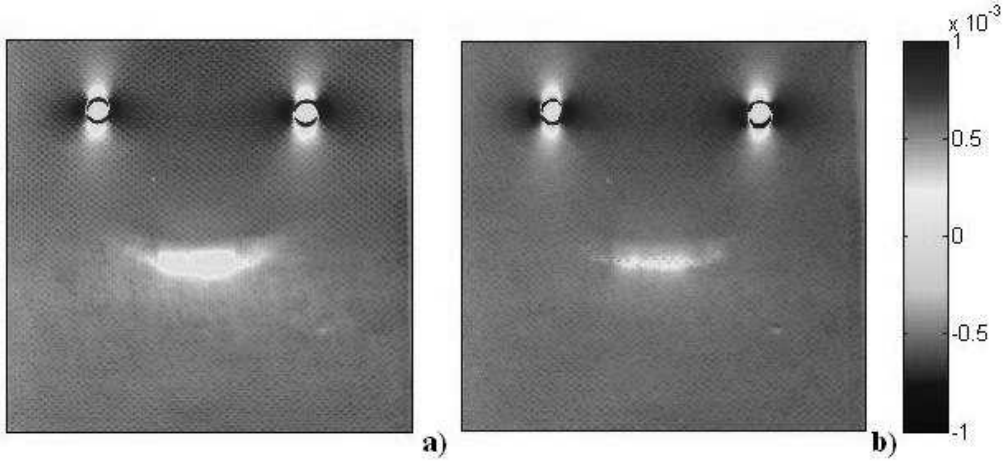

Figure 15: non-dimensional TSA data from damaged WR plate obtained using a) the standard and b) the step load methods

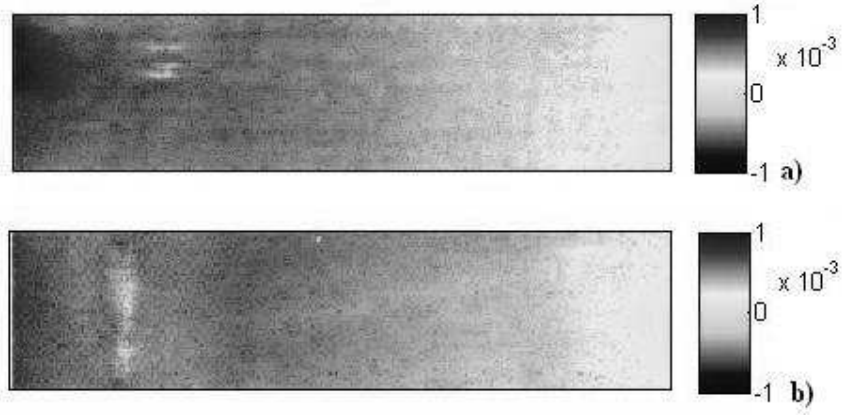

Figure 16: non-dimensional TSA data obtained using the impact method from damaged a) LAM and b) WR materials

Table 1: Materials and manufacturing processes

Specimen	Resin	Reinforcement	Lay-up	Process
UD	(epoxy)	UD fibre	8 (7) plies, 0°	pre-preg (*)
LAM	(epoxy)	UD fibre	$[0,25,-25,0]_S$	pre-preg (*)
WR	Prime 20 LV with fast hardener	plain woven roving 300 gm^{-2}	$[0,25,-25,0]_S$	VARTM (**)
TW	Prime 20 LV with fast hardener	2x2 twill woven roving 500 gm^{-2}	6 plies, 0°	VARTM (**)

(*) Autoclave consolidated pre-impregnated glass fibre matt
(**) Vacuum Assisted Resin Transfer Moulding

Table 2: Material properties for the pre-preg E-glass / epoxy used for materials UD and LAM

E_1	(GPa)	34.2
E_2	(GPa)	10.0
ρ	(kgm^{-3})	1880
C_p	($Jkg^{-1}K^{-1}$)	843
α_1	(K^{-1})	9×10^{-6}
α_2	(K^{-1})	31×10^{-6}